

AD-A100 237

AIR FORCE GEOPHYSICS LAB HANSCOM AFB MA  
SIMULTANEOUS OBSERVATIONS OF AURORAL ZONE ELECTRODYNAMICS BY TW--ETC(U)  
NOV 80 F J RICH, C A CATTELL, M C KELLEY  
AFGL-TR-80-0342

F/G 4/1

NL

UNCLASSIFIED

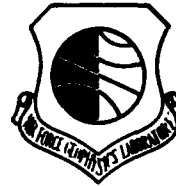
1 of 1  
A100 237


END  
DATE  
FILMED  
7-84  
DTIC

AFGL-TR-80-0342  
ENVIRONMENTAL RESEARCH PAPERS, NO. 719

LEVEL II

12



**Simultaneous Observations of Auroral Zone  
Electrodynamics by Two Satellites: Evidence  
for Height Variations in the Topside Ionosphere**

FREDERICK J. RICH  
CYNTHIA A. CATTELL  
MICHAEL C. KELLEY  
WILLIAM J. BURKE

DTIC  
SELECTE  
JUN 16 1981  
E

10 November 1980

Approved for public release; distribution unlimited.

SPACE PHYSICS DIVISION PROJECT 2311  
**AIR FORCE GEOPHYSICS LABORATORY**  
HANSCOM AFB, MASSACHUSETTS 01731

**AIR FORCE SYSTEMS COMMAND, USAF**



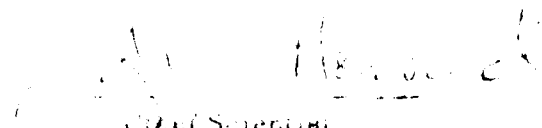
81 6 15 145

DTIC FILE COPY

This report has been reviewed by the Code Information Office (CWO) and is  
releasable to the National Technical Information Service (NTIS).

This technical report has been reviewed and  
is approved for publication.

FOR THE COMMANDER:

  
J. H. Hensley  
Chief Scientist

Approved for release by the Defense Information Security Agency (DISA)  
Dismantling of the Information Center, 10000 Office Building, 10000  
National Technical Information Service.

Unclassified

SECURITY CLASSIFICATION OF THIS PAGE (When Data Entered)

REPORT DOCUMENTATION PAGE		READ INSTRUCTIONS BEFORE COMPLETING FORM
1. REPORT NUMBER AFGL-TR-80-0342	2. GOVT ACCESSION NO. AD-A100 237	3. RECIPIENT'S CATALOG NUMBER
4. TITLE (and Subtitle) SIMULTANEOUS OBSERVATIONS OF AURORAL ZONE ELECTRODYNAMICS BY TWO SATELLITES: EVIDENCE FOR HEIGHT VARIATIONS IN THE TOPSIDE IONOSPHERE.		5. TYPE OF REPORT & PERIOD COVERED Scientific. Interim.
7. AUTHOR(s) Frederick J. Rich      Michael C. Kelley Cynthia A. Cattell      William J. Burke		6. PERFORMING ORG. REPORT NUMBER ERP No. 719
9. PERFORMING ORGANIZATION NAME AND ADDRESS Air Force Geophysics Laboratory (PHG) Hanscom AFB Massachusetts 01731		8. CONTRACT OR GRANT NUMBER(s)
11. CONTROLLING OFFICE NAME AND ADDRESS Air Force Geophysics Laboratory (PHG) Hanscom AFB Massachusetts 01731		10. PROGRAM ELEMENT, PROJECT, TASK AREA & WORK UNIT NUMBERS 14/ 61102F 05 2311/G2 06
14. MONITORING AGENCY NAME & ADDRESS (if different from Controlling Office)		12. REPORT DATE 10 November 1980
		13. NUMBER OF PAGES 35
		15. SECURITY CLASS. (of this report) Unclassified
		15a. DECLASSIFICATION DOWNGRADING SCHEDULE
16. DISTRIBUTION STATEMENT (of this Report)  Approved for public release; distribution unlimited.		
17. DISTRIBUTION STATEMENT (of abstract entered in Block 20, if different from Report)		
18. SUPPLEMENTARY NOTES * Regis College, Weston, Massachusetts † Space Sci. Lab., Univ. of California, Berkeley, California * School of Electrical Eng., Cornell Univ., Ithaca, New York		
19. KEY WORDS (Continue on reverse side if necessary and identify by block number) Aurorae      S3-2 Electric fields      S3-3 Field-aligned currents      Ionosphere Parallel electric fields      Substorms		
20. ABSTRACT (Continue on reverse side if necessary and identify by block number) The S3-2 and S3-3 satellites were launched with identical orbit inclinations and with apogees of 1500 and 8000 km respectively. Both satellites were equipped to measure magnetic fields, electric fields, and energetic electrons. By comparing a few cases when the satellites were crossing the auroral zone at approximately the same universal time and location, altitude variations in the electrodynamics of the auroral zone can be separated from universal and local time variations. Such comparisons show that there are times when the field-aligned current per unit of flux in the auroral zone measured by magnetic		

DD FORM 1 JAN 73 1473

Unclassified

SECURITY CLASSIFICATION OF THIS PAGE (When Data Entered)

4-15-80

Unclassified

SECURITY CLASSIFICATION OF THIS PAGE(When Data Entered)

20. (Cont)

field deflections at the two satellites is the same at both altitudes. There are also times when the field-aligned current per unit of flux is larger at high altitudes than at low altitudes. This requires flow of currents perpendicular to the magnetic field. Comparisons of the convection electric field at the two altitudes show that the electric field does not always map as though field lines were equipotentials. In addition, intense, small-scale (0.1°) electric fields perpendicular to the magnetic field observed at high altitudes are usually not seen in simultaneous low altitude observations. Only in one of the six passes was there a simultaneous observation of a region of intense, small-scale electric fields at 8000 km and 1000 km.

Unclassified

SECURITY CLASSIFICATION OF THIS PAGE(When Data Entered)

## Preface

We wish to acknowledge Dr. M. Smiddy and Mr. B. Shuman of AFGL for providing the S3-2 data; Prof. F.S. Mozer of U.C., Berkeley, for providing the S3-3 data; and Dr. E. Friis-Christensen of the Meteorologisk Institut, Copenhagen, for the Greenland magnetometer data. This work was done under Air Force Geophysics Laboratory contract F19628-80-C-0116, Office of Naval Research contract N00014-75-C-0294, and National Science Foundation grant ATM78-036000.

Accession For	
NTIS GRA&I	<input checked="" type="checkbox"/>
DTIC TAB	<input type="checkbox"/>
Unannounced	<input type="checkbox"/>
Justification	
By	
Distribution	
Availability Codes	
Dist	
A	

## Contents

1. INTRODUCTION	7
2. INSTRUMENTATION	9
3. DATA	12
4. DISCUSSION	24
5. CONCLUSIONS	32
REFERENCES	33

## Illustrations

1. An Example of S3-2 Data Showing the Axial Component of the Magnetic Field Deflection in the Upper Section and the Forward Component of the Convection Electric Field	10
2. Westward Components of the Magnetic Deflections and Southward Components of the Convection Electric Fields Observed Nearly Simultaneously on 3 September 1976 by S3-2 (smooth line) and S3-3 (smooth line with crosses)	13
3. Eastward Components of the Magnetic Deflections and the Northward Components of the Convection Electric Field Observed Nearly Simultaneously in the Dusk Auroral Zone on 6 September 1976 by S3-2 (smooth line with dots) and by S3-3 (smooth line)	15

## Illustrations

4. The Northward Component of the Electric Field as a Function of Invariant Latitude on 6 September 1976 in the Region of the Shock	16
5. Eastward Components of the Magnetic Deflections Observed Nearly Simultaneously in the Noon Sector on 20 September 1977 by S3-2 and S3-3	18
6. Eastward Components of the Magnetic Deflections and Northward Components of the Convection Electric Fields Observed Nearly Simultaneously on 15 October 1976 in the Dusk Auroral Zone by S3-2 (smooth line) and S3-3 (smooth line with crosses)	20
7. Path of S3-2 and S3-3 on 19 September 1976 Projected Along Magnetic Field Lines to 100 km Altitude	21
8. Westward Components of the Magnetometer Deflections and the Southward Components of the Convection Electric Fields for the Nearly Simultaneous Passage Over Greenland by S3-2 (smooth line) and S3-3 (line with dots) on 19 September 1976	21
9. Magnetometer Data From the Greenland Chain Covering the Passage of the Satellites Through the Auroral Zone	22
10. Eastward Components of the Magnetometer Deflections and Northward Components of the Convection Electric Field Observed Nearly Simultaneously on 12 September 1976 in the Dusk Auroral Zone by S3-2 and S3-3	23
11. A Schematic Diagram of the Currents Observed by S3-3 and S3-2 on 19 September 1976	28



# Simultaneous Observations of Auroral Zone Electrodynamics by Two Satellites: Evidence for Height Variations in the Topside Ionosphere

## 1. INTRODUCTION

Field-aligned currents, electric fields, and ionospheric conductivities in the auroral zone have been studied extensively with satellites, rocket and balloon-borne instruments, incoherent scatter radars, and chemical tracers. For example, scanning incoherent scatter radars can be used to map the lowest several hundred kilometers over a latitude range of about 10 degrees. Such scans<sup>1,2</sup> are usually performed near the magnetic meridian and have a time resolution of 5 to 15 minutes. However, it is difficult to determine the dependencies of electric fields and field-aligned currents on latitude, altitude, and magnetic local time. Thus, it is often assumed that Pederson and Hall conductivities are zero and the field-aligned conductivity is infinite above the altitude of the auroral electrojet. This determines the variation of the electric field and field-aligned current with altitude, since magnetic field lines are equipotentials and perfect conductors for field-aligned currents.

(Received for publication 6 November 1980)

1. Horwitz, J. L., Doupnik, J. R., Banks, D. M., Kamide, Y., and Akasofu, S. -I. (1978) The latitudinal distribution of auroral zone electric fields and ground magnetic perturbations and their response to variations in the interplanetary magnetic field, J. Geophys. Res. 83:80.
2. Evans, J. V., Holt, J. M., and Ward, R. H. (1979) Millstone Hill incoherent scatter observations of auroral convection over  $60^\circ \leq T \leq 75^\circ$ , 1., Observing and data reduction procedures, J. Geophys. Res. 84:7059.

There are observations indicating the existence of potential drops along the field line. For example, barium, shaped-charge experiments have successfully "painted" magnetic field lines from 400 km altitude out to many thousands of km, and measured potential differences both parallel and perpendicular to the magnetic fields as a function of altitude.<sup>3, 4, 5</sup> In addition, measurements of ion beams flowing out of the ionosphere and electrons beams into the ionosphere by the S3-3 satellite<sup>6-13</sup> tend to confirm the existence of electric potential drops along magnetic field lines at altitudes near and below  $\sim 1R_p$ . Electric field measurements from the S3-3 satellite suggest that parallel electric fields exist on two scale sizes.<sup>12</sup> Latitudinally narrow ( $\leq 0.1^\circ$ ) regions of the strong perpendicular electric fields<sup>14</sup> have been identified as the signatures of electrostatic shocks.<sup>15, 16</sup> Direct observations of the parallel electric fields in some shocks have been made.<sup>12</sup> Therefore, the assumption that magnetic field lines are equipotentials is not always valid in the region of shocks. In addition, Mozer and Torbert<sup>17</sup> have presented evidence for the existence of parallel electric fields between 1000 and 8000 km in the auroral zone over a latitudinal region of several degrees. They found that the total potential drop across the auroral zone is independent of altitude, but that the equipotentials do not follow field lines.

Such data require a reassessment of the assumption that the Pederson and Hall conductivities are approximately zero and that the field-aligned conductivity is infinite above the auroral electrojet. The validity of this assumption is supported on a large scale by the observation that the patterns of convection electric fields observed in the auroral zone and the magnetosphere are similar. They are certainly of the correct order of magnitude when compared. A direct study of the outer plasmaspheric electric field in the magnetosphere (via whistles) and ionosphere (via radar) showed excellent agreement with the mapping hypothesis even in disturbed times.<sup>18</sup> On the other hand, the observations have indicated the existence of potential drops along field lines which in turn require a breakdown in the equipotential structure on some scale in the auroral zone. Swift<sup>15, 16</sup> and Kan and Lee<sup>19</sup> have suggested V- or S-shaped structures for the equipotentials in the region of parallel electric fields or double layers. The strong, latitudinal, thin regions of potential drops associated with electrostatic shocks by Mozer et al<sup>14</sup> are apparently the sides of such V- or S-shaped potential structures.

In this report, we investigate the assumption that the field-aligned current in a flux tube is independent of altitude by comparing nearly simultaneous magnetic field observations from the S3-2 and S3-3 satellites. This investigation is undertaken to provide a clearer understanding of height variations than can be obtained by comparing passes from the same or diverse satellites and/or rockets made

(Due to the large number of references cited above, they will not be listed here. See References, page 33.)

at widely different times. Simultaneous dc electric field measurements are also presented to provide evidence for parallel electric fields by showing the failure of the magnetic field lines to be equipotentials. An example of simultaneous observations of intense dc electric fields by both satellites illustrates height variations of shocks. Section 2 describes the instrumentation, data analysis, and the format of the data. Section 3 presents the data and describes the comparisons. Section 4 discusses theoretical explanations for the observed height variations of field-aligned currents and electric fields and consequences of these variations for the coupling of the magnetosphere and ionosphere.

## 2. INSTRUMENTATION

The S3-2 satellite was launched in December 1975 into a  $96.3^\circ$  inclination orbit with an initial apogee and perigee of 1557 km and 240 km respectively. It was spin stabilized in a cartwheel mode with a nominal spin period of 20 seconds. The orbit plane drifted westward in local time approximately 0.5 hour per month. The scientific package used for auroral studies has been described by Burke et al.<sup>20</sup> The scientific package used for this study consist of a dc electric field instrument, a triaxial fluxgate magnetometer, and an energetic electron spectrometer. The electric field instrument consists of one dipole probe in the spin plane and one along the spin axis. Although data are output 32 times per second, the electric field vector components in the spin plane generally are determined from fitting a quarter of a spin period. The component along the axis of the satellite is often unusable because of unknown level shifts due to changes in the chemistry of the environment, which is quite variable in the auroral zone below  $\sim 1000$  km altitude. The magnetometer outputs the components of the magnetic field 32 times per second with a resolution of 5 nT. The magnetometer changes ranges each time the magnetic field along an axis changes by 1000 nT. During a range change approximately two measurements along that axis are lost. Since the magnetometer along the spin axis (referred to as  $B_{XS}$ ) has many fewer range changes per spin period (especially near perigee), the temporal resolution of the magnetic deflection component along the spin axis is the best of the three components. The IGRF75 model magnetic field is subtracted from the three measured components obtained by the magnetometer. The resulting magnetic deflections are due to spacecraft fields of  $\sim 100$  nT or less, uncertainties in the model field of  $\sim 500$  nT or less, and field-aligned currents.

20. Burke, W.J., Hardy, D.A., Rich, F.J., Kelley, M.C., Smiddy, M., Shuman, B., Sagalyn, R.C., Vancour, R.P., Wildman, P.J.L., and Lai, S.T. (1980) Electrodynamic structure of the late evening sector of the auroral zone, J. Geophys. Res. 85(A3):1179-1193.

By fitting the data to smooth baselines, the first two components of the magnetic deflections can be removed. The electron spectrometer obtains a spectrum of electrons in the range of 80 eV to 17 keV once per second. The low geometric factor of the spectrometer makes it insensitive to weak fluxes of precipitating electrons, especially below 1 keV.

Figure 1 shows an example of data from S3-2 taken over the morning sector of the northern polar cap and auroral zone.  $\Delta B_{XS}$  is the axial component of the magnetic field deflection. Over the north pole,  $\Delta B_{XS}$  is eastward (westward) on the dusk (dawn) side. Positive (negative) slopes of  $\Delta B_{XS}$  as plotted represent field-aligned currents into (out of) the ionosphere. Due to the alignment of the satellite,  $\Delta B_{XS}$  is nearly equal to the east-west component of the magnetic field deflection, the major component of magnetic deflections caused by field-aligned currents in the auroral zone. In most cases in this report, the actual east-west component of the deflection has been plotted in a manner similar to  $\Delta B_{XS}$  in Figure 1 so that positive (negative) slopes represent currents into (out of) the ionosphere. The bottom panel shows the forward component of the dc electric field after subtracting the corotation field. The forward component of the electric field is approximately northward (southward) on the dusk (dawn) side. Positive (negative) values of the forward component of the electric field represents sunward (anti-sunward) convection when the satellite is crossing the pole through the dusk-dawn sector.

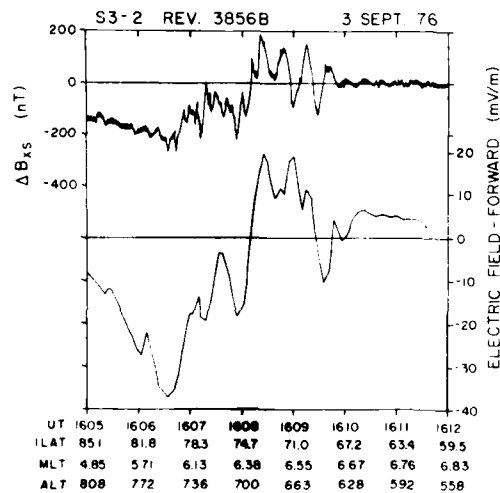


Figure 1. An Example of S3-2 Data Showing the Axial Component of the Magnetic Field Deflection in the Upper Section and the Forward Component of the Convection Electric Field. The axial component of  $\Delta B$  is approximately westward (eastward) and the forward component of  $E$  is approximately southward (northward) on the dawn (dusk) side of the north pole.

The S3-3 satellite, which is instrumented similar to the S3-2 satellite, was launched in July 1976 into a 97.5° inclination orbit with an initial apogee and perigee of 8040 and 240 km respectively. The S3-3 satellite is also spin stabilized in a cartwheel mode with a nominal spin period of 20 seconds. During the period of September–October 1976, the two satellites were nearly coplanar in the dusk-dawn sector, and during the period October–December 1977, the two satellites were nearly coplanar in the noon-midnight sector.

The electric field experiment and magnetometer on S3-3 are described by Mozer et al.<sup>21</sup> The triaxial fluxgate magnetometer has two gain states whose full outputs are  $\pm 60,000$  nT and  $\pm 10,000$  nT, and one bit resolution of 480 nT and 80 nT respectively with readouts four times per second. By averaging the data over a spin period, a resolution of  $\sim 10$  nT for the magnetic deflection can be obtained with a temporal resolution of  $\sim 20$  seconds. The dc electric field experiment is similar to the S3-2 experiment. The principal difference is that there are two orthogonal dipole probes deployed in the spin plane of S3-3 compared to a single dipole in the spin plane of S3-2. Both satellites have dipoles along their spin axis. Thus the dc electric field vector can be obtained eight times per second on S3-3. To remove variations due to turbulence and instrumental effects, the electric field data shown herein have been averaged over a spin period. Electric field variations due to electrostatic shocks are shown by annotation only (with the exception of Figure 4). The energetic particle experiments on S3-3 are described by Sharp et al.<sup>9</sup> and Mizera and Fennell.<sup>6</sup>

In order to compare the measured electric and magnetic field parameters for S3-2 and S3-3, it is necessary to scale the data in a manner that compensates for the decrease in electric field and field-aligned current due to the divergence of magnetic field lines with altitude. We have done this by generalizing the scaling algorithm of Mozer.<sup>22</sup> The east/west component of the electric field scales as:

$$E_{ew}(r_1)/E_{ew}(r_2) = (r_2/r_1)^{3/2} = r^{3/2} \quad (1)$$

where  $r_1$  and  $r_2$  are two radial distances from the center of the earth along the same field line. The north/south component of the electric field scales as:

$$E_{ns}(r_1)/E_{ns}(r_2) = r^{3/2} \left(1 - \frac{3r_1}{4L}\right)^{1/2} / \left(1 - \frac{3r_2}{4L}\right)^{1/2} \quad (2)$$

21. Mozer, F.S., Cattell, C.A., Tererin, M., Torbert, R.B., Vonglinski, S., Woldorf, M., and Wygant, J. (1979) The dc and ac electric field, plasma density, plasma temperature and field aligned current experiments on the S3-3 satellite, J. Geophys. Res. 84(A10):5875-5884.

22. Mozer, F.S. (1970) Electric field mapping in the ionosphere at the equatorial plane, Planet. Space Sci. 18:259-263.

where  $L$  = McIlwain parameter =  $R_e \cos^{-1/2}$  (Inv. Latitude). We assume that the magnetic field deflections are minor perturbations of the main field and due only to semi-infinite current sheets aligned in the east/west direction. Then, assuming that the currents are constant along the flux tube, the deflections scale as the east/west component of the divergence in the magnetic field, or:

$$\Delta B_{ew}(r_1)/\Delta B_{ew}(r_2) = r^{3/2}. \quad (3)$$

### 3. DATA

We have found over 150 instances when the two satellites simultaneously passed within a few degrees of each other in invariant latitude/magnetic local time coordinates. Of these possible data sets, we studied 12 that were immediately available. Most of these simultaneous passes were obtained in September–October 1976 when the two satellites were approximately coplanar. One September 1977 pass occurred when the two satellites were separated by 2.5 hours of local time. Only six of the passes were suitable for this study. Of the rejected passes, four were east-west passes through the dayside cusp region and two were unusable because the data quality was poor. There is a degree of bias in the selection of data toward active periods for several reasons: More observations were made during active periods than during quiet periods. Also, during active periods, the field-aligned currents are larger and easier to distinguish. Since the structure of the auroral zone is often changing rapidly during active periods, available ground magnetograms were examined to determine whether or not the differences between the two satellite's observations were temporal.

The first example of nearly simultaneous passes is a dawn pass from the polar cap through the auroral zone to the plasmasphere (Figure 2). The S3-2 data are the same as in Figure 1, except that some of the small-scale features are not shown in Figure 2. This was done to make it easier to plot the data with invariant latitude instead of time as the ordinate. On the other hand, all the available data from S3-3 are shown due to the requirement of spin averaging. Both satellites observed the auroral zone field-aligned currents between  $74^\circ$  and  $67^\circ$  invariant latitude. The ionospheric production region in both the polar cap and auroral zone was sunlit. As described by Smiddy et al.<sup>23</sup> for "summer-like" conditions, the east-west magnetic field deflection changes correspond to changes in the north-south component of the

23. Smiddy, M., Burke, W.J., Kelley, M.C., Saflekos, N.A., Gussenhovorn, M.S., Hardy, D.A., and Rich, F.J. (1980) Effects of high latitude conductivity on observed convection electric fields and Birkland currents, J. Geophys. Res. 85(A12):6811-6818.

convection electric field. The electric and magnetic field reversal are clearly seen in Figure 1. The current sheets observed by both satellites in the auroral zone and the polar are complex. While details of the currents observed by the two satellites do not match, the general size and location of the current sheets do match.

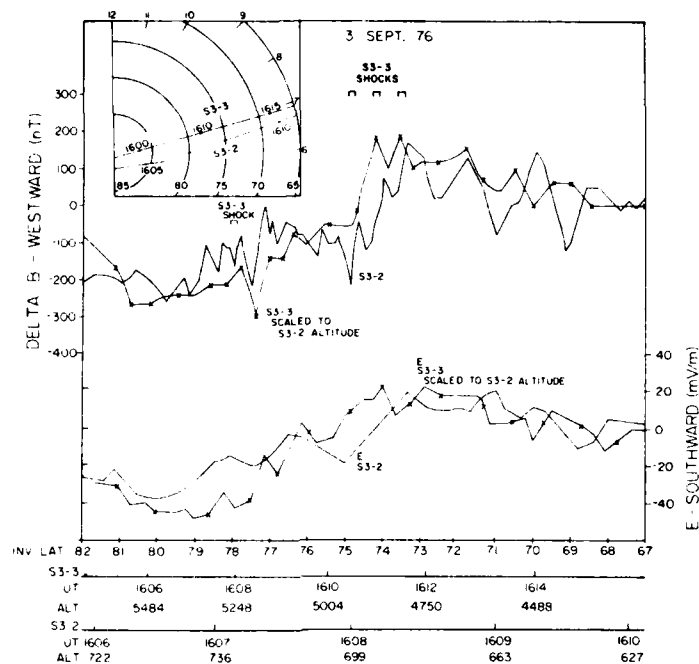


Figure 2. Westward Components of the Magnetic Deflections and Southward Components of the Convection Electric Fields Observed Nearly Simultaneously on 3 September 1976 by S3-2 (smooth line) and S3-3 (smooth line with crosses). The S3-3 components have been scaled to the S3-2 altitude so that equivalent sheet currents will give equivalent deflections; the statistical error of the S3-3  $\Delta B$  is  $\pm 20\gamma$ . The inset shows the path of the two satellites in invariant latitude-magnetic local time coordinates. The hourly coverage of the interplanetary magnetic field for this period was -1.7, 0.4, 2.0 nT, and Kp was 2

An examination of the electric field data shows a region of latitudinally narrow ( $\leq 0.1$ ), intense ( $E \geq 100$  mV/m) dc electric fields near 1608 UT and three such regions between 1610 and 1611 UT. We refer to all such regions of narrow, intense

dc electric field perpendicular to the magnetic field as "shocks" whether or not there is any indication of an electric field component parallel to the magnetic field. If there is no component parallel to the magnetic field, the structure is a laminar shock; if there is a component parallel to the magnetic field, the structure is a V- or S-shaped shock or an extended double layer. An examination of the simultaneous S3-2 data shows no evidence of shocks near 700 km altitude. This tends to confirm the geometry of shock structures suggested from the statistics of occurrence frequency and electric field strengths observed by S3-3 and ISEE (Mozer et al,<sup>14</sup> Torbert and Mozer,<sup>24</sup> Mozer<sup>25</sup>). The shock extends from the equatorial plane to ~8000 km altitude as a laminar shock and then terminates between ~8000 km and ~2000 km as a V-shaped shock. The shock near 78° invariant latitude is close to a structure that could be the signature of a polar cap arc. Since the field lines in the polar cap are open, the shock structure would map onto the magnetopause. The shocks between 75° and 73° are in the region 1 auroral zone current system, and they should map to the equatorial plane of the magnetosphere.

A comparison of the particle data from both satellites was made near the shock regions. The peak in the energy spectrum is at the same energy for both satellites. This is consistent with little or no particle acceleration between the satellites in the region of the shocks. However, the two-particle data sets show a 1 keV difference in the peak of the energy spectra near 79° invariant latitude. The flux observed by S3-3 peaked near 1 keV, and the flux observed by S3-2 peaked near 2 keV. This implies a parallel potential drop where no shock was observed. It is impossible to tell whether this one observation was due to an acceleration region that was wholly between the two satellites altitudes.

Figure 3 is another examples of nearly uniform structure at the two satellite altitudes as they passed each other in the dusk auroral zone. The equatorward, or region 2, field-aligned current is very weak. There is a difference of approximately 2.5° in the location of the region 1 current system, but, after considering the separation of approximately 1 hour in local time between the satellites, this can be attributed to the increasing latitude of the auroral zone as one approaches the day side.

A significant feature of the observations from both satellites is the existence of strong, dc electric fields oriented primarily perpendicular to the geomagnetic field in the north-south direction. Following the convention stated above, these electric field features are called shocks, and it is assumed that they are part of an

24. Torbert, R.B., and Mozer, F.W. (1978) Electrostatic shocks as the source of discrete auroral arcs, Geophys. Res. Letters 5(No. 2):135-138.
25. Mozer, F.W. (1980) ISEE-1 observations of electrostatic shocks on auroral zone field lines between 2.5 and 7 Earth Radii, submitted to Geophys. Res. Letters.



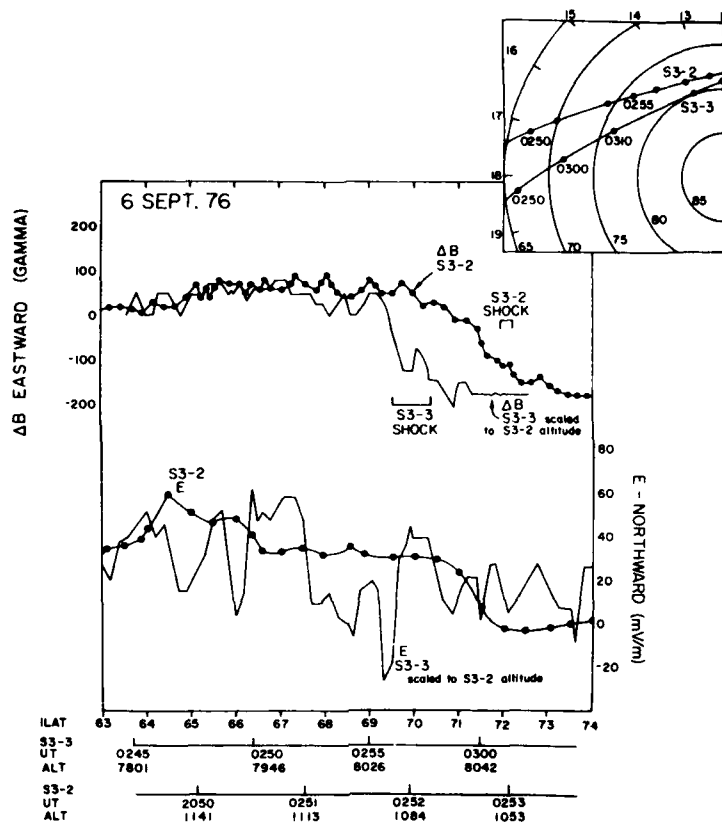


Figure 3. Eastward Components of the Magnetic Deflections and the Northward Components of the Convection Electric Field Observed Nearly Simultaneously in the Dusk Auroral Zone on 6 September 1976 by S3-2 (smooth line with dots) and by S3-3 (smooth line). The statistical error of the S3-3  $\Delta B$  is  $\pm 27 \gamma$ . No IMF data is available for this period. Kp was 3

electrostatic shock structure as proposed by Swift<sup>15</sup> and Hudson and Mozer.<sup>26</sup> These "shocks" are embedded in a wider region of low frequency ( $\sim 100$  Hz) turbulence. The strong dc electric fields or shocks (Figure 4) are more complex than what would be expected from a simple V- or S-shaped shock. After aligning the region 1 current systems from the two satellites, we find that the shock region observed by S3-3 is approximately aligned with the shock region observed by S3-2.

26. Hudson, M.K., and Mozer, F.W. (1978) Electrostatic shocks, double layers, and anomalous resistivity in the magnetosphere, Geophys. Res. Letters 5:131.

The details of the dc electric field structure do not map one-to-one from one satellite to the other. If we assume that these shock regions are two parts of a single structure, then the region of the shocks must extend at least 7000 km in altitude and 1 hour in local time, and perhaps much more, as has been previously suggested by Mozer et al<sup>12</sup> on the basis of the relative magnitudes of the north-south and the east-west components of the electric field. The shock region is wider and the electric fields are stronger at the high altitudes. This change in the strength of  $E_{\perp}$  with altitude is another indication of a parallel electric field. Mizera et al<sup>27</sup> examined the particle data in this shock region and found evidence for parallel electric fields through the region from 69° to 71° inv. lat. based on upflowing ion beams and downflowing electron beams.

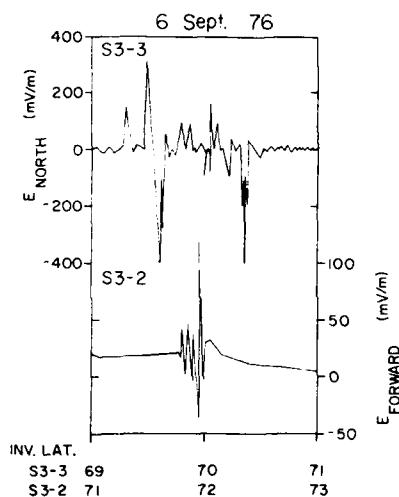


Figure 4. The Northward Component of the Electric Field as a Function of Invariant Latitude on 6 September 1976 in the Region of the Shock. The upper portion shows the electric field observed by S3-3 and the lower portion shows the electric field observed by S3-2

Of the data sets examined so far, the simultaneous pass on 6 September 1976 is the only example of a shock region being observed simultaneously at high and low altitude. Since the S3-3 satellite observed shocks more often near apogee (~8000 km) than at other altitudes (Mozer et al<sup>25</sup>) and S3-2 with an apogee of 1500 km seldom observed shocks, we conclude that regions of strong dc electric fields with narrow latitudinal extent do not usually penetrate to altitudes less than ~1500 km.

27. Mizera, P.F., Fennell, J.F., Croley, D.R., Jr., Vampola, A.L., Mozer, F.S., Torbert, R.B., Tenerin, M., Lysak, R., Hudson, M., Cattell, C.A., Johnson, R.J., Sharp, R.D., Ghielmetti, A., and Kintner, P.M. (1980) The aurora inferred from S3-3 particles and fields, submitted to J. Geophys. Res.

The S3-3 pass shown in Figures 3 and 4 was studied in detail by Mizera et al<sup>27</sup> who describe the waves and particles associated with the shock. An inverted V event was colocated with the shock structure as were intense coherent ion cyclotron waves and a region of broadband low frequency noise with wave fields as large as 20 mV/m. The S3-2 data are nearly identical in form but limited to a smaller range of invariant latitude. Unfortunately, wave measurements were not available on S3-2. A crude measure of the ion composition is possible from S3-2 data, using the ratio of the ram to wake current measures by a thermal ion detector on the vehicle (Smiddy et al<sup>28</sup>). On the 6 September 1976 orbit, the composition changed from primarily  $O^+$  with less than 10%  $H^+$  to an ionosphere with  $40\% \pm 25\%$   $H^+$  very near the shock-like structure, with the hydrogen-rich composition in the poleward region. The density of thermal ions was well below the sensitivity of the detector on S3-3, but the super thermal-ion ( $E \geq 500$  eV) detector observed only  $H^+$  throughout the region of the shocks.

Although they are not shown in Figure 3, there are a pair of field-aligned sheet currents of opposite current flow directions and equal magnitudes associated with the shock observed by S3-2. The current sheets are  $\sim 5$  km in latitude extent and carry a sheet current of  $\sim 40$  mA/m. The S3-3 magnetometer does not have sufficient resolution to find such small-scale current sheets that may be associated with shocks. Hardy et al<sup>29</sup> found that small-scale current sheets are generally observed near shocks observed by S3-2.

Figure 5 shows an example of a simultaneous pass through the afternoon auroral zone by the two satellites with a local time separation of 2.5 hours. The S3-2 electric field data are also shown to indicate that S3-2 did not enter the polar cap region until reaching  $77^\circ$  invariant latitude. The S3-3 electric field data indicate that it crossed the polar cap boundary at  $73^\circ$ . Although there is a great deal of difference in the latitudinal profile of the field-aligned current system between the two satellites, the total sheet current observed in both parts of the afternoon sector is the same. The difference in the latitude of the two observations of the current sheets and the latitudinal width of the sheets are typical of the shape of auroral oval and the average distribution of field-aligned currents presented by Iijima and Potemra.<sup>30</sup> The region 2 current observed by S3-2 shows a great deal

28. Smiddy, M., Kelley, M. C., Burke, W., Rich, F., Sagalyn, R., Shuman, B., Mays, R., and Lai, S. (1977) Intense pole-ward directed electric fields near the ionospheric projection of the plasmopause, Geophys. Res. Letters 4:543.

29. Hardy, D. A., Burke, W. J., Rich, F., and Kelley, M. C. (1980) Intense Birkeland Current structures observed in the vicinity of latitudinally narrow dc electric field variations, to be submitted to J. Geophys. Res.

30. Iijima, T., and Potemra, T. A. (1976) The amplitude distribution of field-aligned currents at northern high latitudes observed by TRIAD, J. Geophys. Res. 81(No. 13):2165-2174.

of small-scale structure due to the closeness of the observations to the dayside cusp, but the large-scale patterns are clearly discernable. Thus, there is little doubt that both satellites were observing the afternoon sector of the auroral zone. The similarity of the observed sheet currents suggest that the auroral zone sheet currents were nearly constant in strength across a span of at least 2.5 hours of local time. This is contrary to the average current observed by TRIAD, which is ~20% greater near 1500 local time than near 1300 local time; thus, the average sheet current is ~30% to ~50% greater.

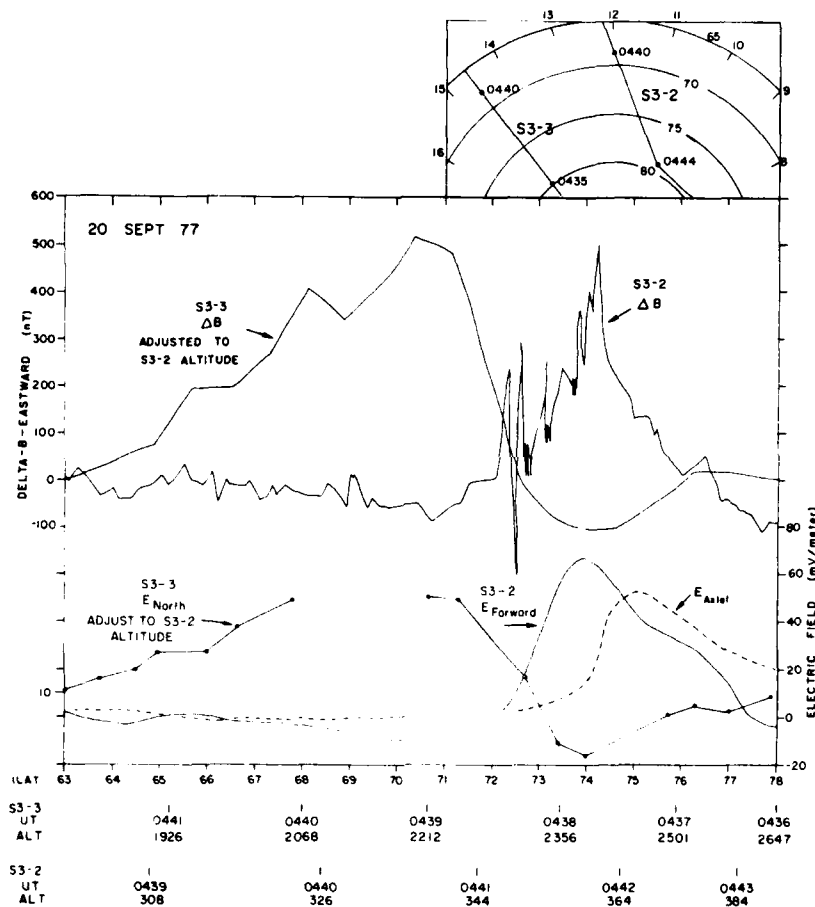


Figure 5. Eastward Components of the Magnetic Deflections Observed Nearly Simultaneously in the Noon Sector on 20 September 1977 by S3-2 and S3-3. The statistical error of the S3-3  $\Delta B$  is  $\pm 85 \gamma$ . The forward and axial components of the S3-2 convection electric field and the northward component of the S3-3 convection electric field are shown in the bottom section of the panel. No IMF data is available for this period.  $K_p$  was 5.

We now turn our attention to some cases where the sheet currents observed by the two satellites are clearly different. The first example is the passage through the dusk auroral zone by the two satellites on 15 October 1976 (Figure 6). The satellites were separated by 0.5 hour in local time, which accounts for a  $0.7^\circ$  difference in the latitude of entry into the polar cap. The two satellites entered the auroral zone simultaneously, but S3-2 left the auroral zone 11 minutes ahead of S3-3. The most striking feature of this passage is that S3-3 observed almost four times more sheet current than S3-2. Since this period was magnetically active, ground magnetometer records were examined. They show an increase in the auroral electrojet at approximately the time of the passage. Thus, the sheet current may have strengthened significantly during the few minutes between the passage of S3-2 and S3-3. However, the degree of strengthening in the currents does not match the magnitude of the strengthened electrojet change observed at the standard magnetometer stations. We are left with a change in the sheet current, which may be either temporal or spatial, despite the fact that the passage of the two satellites was nearly simultaneous. There were some differences in the observations that would seem to be related to height. There are electrostatic shocks observed by S3-3, but not by S3-2. Also, the S3-3 particle data show upflowing ion beams in the region of the shocks that is evidence for a parallel electric field between the two satellites.

Another example of the magnitudes of the field-aligned sheet currents not matching was observed on 19 September 1976. The two satellites crossed the morning auroral zone with little separation in local time and very close to the Greenland magnetometer chain, as shown in Figure 7. The data were obtained in the middle of a substorm that has been modelled by Harel et al.<sup>31,32</sup> The electric and magnetic field data from S3-2 and S3-3 are shown in Figure 8. S3-3 passed through the auroral zone 5 minutes before S3-2 and observed a larger and latitudinally broader sheet current and convection electric field than did S3-2. The location of the polar cap-auroral zone boundary observed by S3-3 was  $0.5^\circ$  equatorward of the location observed by S3-2. An examination of the ground-based magnetometer data (Figure 9) indicates that the auroral electrojet was slightly poleward of Frederikshåb and moving poleward at the time of the satellite passage. The magnitude of the auroral electrojet does not seem to change significantly during this period, since a recovery of the H component of Frederikshåb is approximately equivalent to the decrease in the H component at Godthåb. We conclude that the ground-based data

31. Harel, M., Wolf, R.A., Reiff, P.H., Spiro, R.W., Burke, W.J., Rich, R.J., and Smiddy, M. (1980) Quantitative simulation of a magnetospheric substorm, 1. Model logic and overview, submitted to J. Geophys. Res.
32. Harel, M., Wolf, R.A., Spiro, R.W., Reiff, P.H., Chen, C.K., Burke, W.J., Rich, R.J., and Smiddy, M. (1980) Quantitative simulation of a magnetospheric substorm, 2. Comparison with observations, submitted to J. Geophys. Res.

supports the hypothesis that the location of the auroral zone moved during the interval between the two satellite observations, but the magnitudes of the sheet currents and electric field did not undergo a temporal change. Thus, a height variation in these parameters is suggested, although temporal changes cannot be completely ruled out.

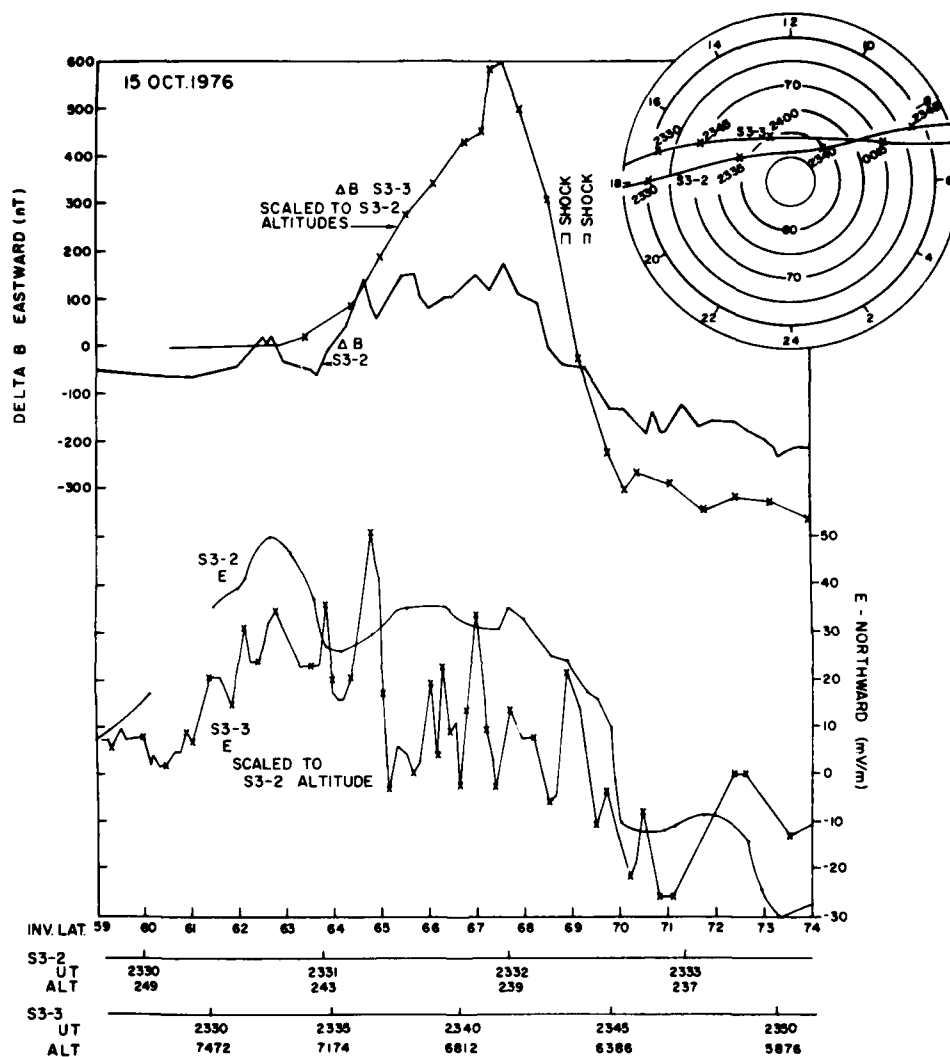


Figure 6. Eastward Components of the Magnetic Deflections and Northward Components of the Convection Electric Fields Observed Nearly Simultaneously on 15 October 1976 in the Dusk Auroral Zone by S3-2 (smooth line) and S3-3 (smooth line with crosses). The statistical error of the S3-3  $\Delta B$  is  $\pm 29 \gamma$ . The insert shows the path of the two satellites across entire northern, high latitude region. IMF was not available for this period. Kp was 4

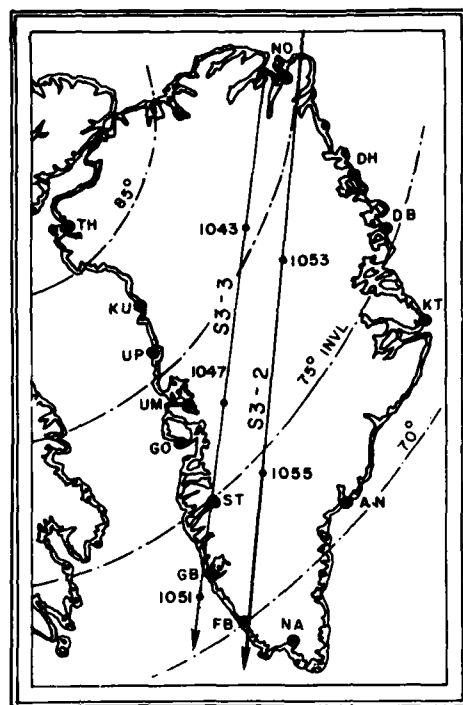


Figure 7. Path of S3-2 and S3-3 on 19 September 1976 Projected Along Magnetic Field Lines to 100 km Altitude. The stations used for this study are ST (Sndre Strmfjord), GB (Godthåb), FB (Frederikshåb), and NA (Nassarssuag). Magnetic Local Time at these stations is GMT minus 2 hours

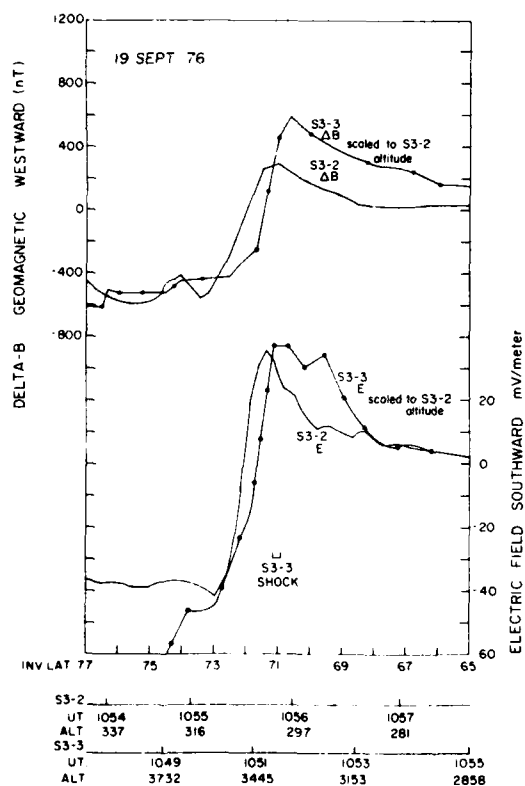


Figure 8. Westward Components of the Magnetometer Deflections and the Southward Components of the Convection Electric Fields for the Nearly Simultaneous Passage Over Greenland by S3-2 (smooth line) and S3-3 (line with dots) on 19 September 1976. The statistical error of the S3-3  $\Delta B$  is  $\pm 20 \gamma$ . IMF was not available. Kp was 4<sup>+</sup>

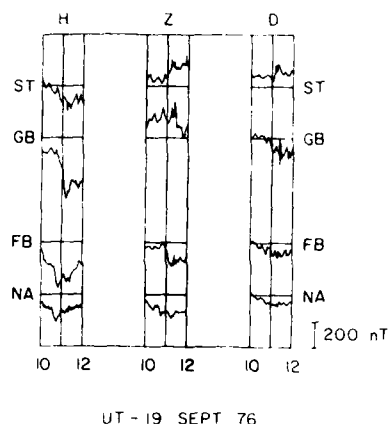


Figure 9. Magnetometer Data From the Greenland Chain Covering the Passage of the Satellites Through the Auroral Zone

It is interesting to note that, if the convection electric field data are moved so that the polar cap boundaries match, the electric fields are almost identical throughout the region of downward current and that the peak values of the electric field are also identical and occur at the same location. However, the electric fields disagree throughout the upward current region, suggesting that there is a parallel electric field between the two satellites. The S3-3 high-time resolution of electric-field data shows an electrostatic shock that was not observed by S3-2. In this case, there is no evidence in the S3-3 data for a parallel electric field associated with this shock, in agreement with the suggestion of Cattell et al.<sup>33</sup>

A final example of unequal sheet currents observed by the two satellites is shown in the dusk auroral zone in Figure 10. Not only does the S3-3 observe approximately 50% more sheet current, but the latitudinal profile of the field-aligned current is significantly different. The region 2 current observed by S3-3 flows entirely between 70° and 71°, while it is observed by S3-2 from 70° to 73°. The precipitating electron data also show a difference between the two satellites. S3-3 encountered precipitating electrons poleward of 71°, and S3-2 encountered precipitating electrons poleward of 73°. Since there is a delay of 5 to 8 minutes between the passage of the two satellites, we have considered the possibility that the observed difference is due to a temporal change. Ground-based magnetometers indicate that this observation was made during a quiet period between two small substorms. One substorm was 1.5 hours earlier and one was 1.5 hours later. We conclude that the variation between the two satellites was more likely to be spatial

33. Cattell, C., Lysak, R., Torbert, R. B., and Mozer, F. S. (1979) Observations of differences between regions of current flowing into and out of the ionosphere, *Geophys. Res. Letters* 6(No. 7):621-624.



than temporal. This means that the region 2 field-aligned current was significantly altered between 1000 km and 8000 km altitude. This would of course require current to flow across field lines in this altitude range. The S3-3 particle data provide evidence for the existence of a parallel electric field below the S3-3 satellite in the region of upward (region 1) current.

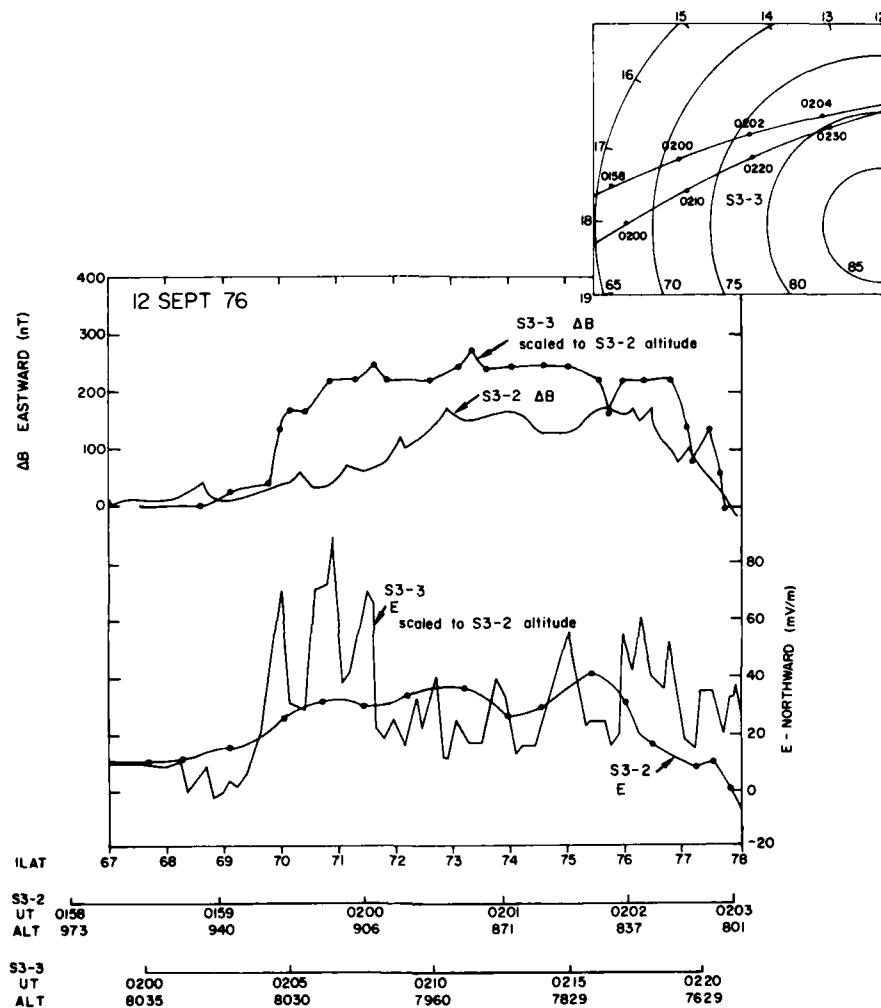


Figure 10. Eastward Components of the Magnetometer Deflections and Northward Components of the Convection Electric Field Observed Nearly Simultaneously on 12 September 1976 in the Dusk Auroral Zone by S3-2 and S3-3. The S3-3 ΔB-east and S3-2 E-north are shown as lines with dots. The statistical error of the S3-3 is ΔB is  $\pm 27 \gamma$ . The insert shows the path of the two satellites in invariant latitude-magnetic local time coordinates. The IMF was 2.0, 4, 8, and 1.8 nT for 02-03 UT. Kp was 2<sup>-</sup>

#### 4. DISCUSSION

We have presented magnetic and electric field data from six near conjunctions of the S3-2 and S3-3 satellites. These observations give preliminary evidence for answering the following questions about auroral electrodynamics: Are there altitude variations in the field-aligned currents in a flux tube between 8000 km and the auroral electrojet? What is the altitude profile of the electrostatic shock electric fields? What, if any, is the relationship between electrostatic shocks and field-aligned currents? Are there systematic variations in the convection electric field with altitude?

Regions of strong dc electric fields perpendicular to the magnetic field, which are referred to as shocks, are not seen very often at S3-2 altitudes, but the shock observed by S3-2 on 6 September 1976 at 1000 km is probably part of a region of shocks observed by S3-3 at 8000 km altitude. Thus, the shocks that are seen by S3-2 are the low altitude tips of shocks that extend to great heights. The fact that shocks are rare in the S3-2 observations and common in the S3-3 observations near apogee means that most shocks terminate above 1500 km. For example, we can say that the shocks seen by S3-3 on 3 September 1976 (Figure 2) terminated above 700 km. This has been previously suggested by an altitude dependence of the occurrence frequency of shock observations by S3-3 (Mozer et al<sup>12</sup>).

In order for the strong perpendicular electric fields in shock regions to terminate above 1500 km, there must be a region where there is a parallel component of the electric field in the shock structure to form a V- or S-shaped shock or extended double layer, as suggested by Swift.<sup>15, 16</sup> Mozer et al<sup>12</sup> made direct observations of parallel electric fields in the region of strong perpendicular electric fields. The altitude distribution of the parallel electric field has been suggested by particle measurements (Ghielmetti et al,<sup>10</sup> Gorney et al<sup>13</sup>). Upward directed electric fields accelerate ions into upward directed beams and electrons into downward directed beams. Ghielmetti et al<sup>10</sup> concluded that the acceleration of particles (and thus the region of parallel electric fields) generally extended from ~4000 km to greater than 8000 km. Mozer<sup>25</sup> using both S3-3 and ISEE data, concluded that the region of parallel fields is generally between altitudes of a few thousand km and ~12,000 km.

The next question that arises is what causes the parallel electric fields that should collocate with the region of strong perpendicular electric fields? The data from the S3-2 thermal ion trap suggests that a chemistry change in the ionosphere may be partially responsible for the termination of the shock. If we assume that oxygen ( $O^+$ ) and hydrogen ( $H^+$ ) are the only thermal components of the topside ionosphere, we find no significant component of hydrogen ( $H^+ < 10\%$ ) in the

auroral zone equatorward of the shock. Immediately poleward of the shock, there is a significant, but not dominant, component of hydrogen ( $H^+ \sim 25-50\%$ ). The region of parallel electric fields or double layer may be related to the local ion mass. Hence, the location of the shock on 6 September 1976 at S3-2 altitude may have been determined by a latitudinal gradient in the ion composition. Specifically, the oxygen-rich region near the S3-2 shock may have been unstable due to strong plasma turbulence, which is related to the formation of a double layer, but the higher latitude region containing more hydrogen was not unstable.

There are theoretical suggestions for the formation of regions of parallel electric fields which include predictions for the lower and upper altitude boundaries for these regions. Lysak and Hudson<sup>34</sup> have suggested that regions of parallel electric fields are current-driven instabilities that dissipate the energy in Alfvén waves propagating toward the ionosphere from the magnetosphere and plasma sheet. The region of parallel electric fields occurs where the electron drift velocity associated with the field-aligned currents is maximum, that is, where  $B/n$  is maximum. Observations of beams of upflowing ions, ion distributions peaked along the field line, are only found in regions of upward current (Cattell et al.<sup>33</sup>). Since ion beams mark the presence of parallel electric fields, these observations indicate that parallel electric fields pointed upward are only found where downward flowing magnetosphere electrons are carrying the field-aligned current. The fact that the electron drift velocity at the altitude of S3-2 is significantly less than at the S3-3 altitude ( $B/n \approx 1 \times 10^{-4} \text{ G.cm}^3$  and  $6 \times 10^{-3} \text{ G.cm}^3$ , respectively) seems to disagree with the mechanism of Lysak and Hudson.<sup>34</sup> However, the perpendicular electric field in the shock region is smaller by a factor of 4 at the S3-2 altitude than at the S3-3 altitude. This implies that most of the region of parallel electric fields is above the S3-2 altitude.

Kan and Lee<sup>19</sup> have suggested that the lower boundary of parallel electric fields occurs in the region where the upward drift of ionospheric ions, that is, the polar breeze or polar wind, goes supersonic. The S3-2 drift meter does not indicate a supersonic field-aligned flow. However, the S3-2 drift meter tends to respond to the dominant component of the ambient plasma. If  $H^+$  is a minor component in the region of the shock and is supersonic, the conditions suggested by Kan and Lee<sup>19</sup> are satisfied.

Regions of strong perpendicular electric or shock fields may be related to inverted V events and discrete auroral arcs. Inverted V's are regions with  $\sim 1^\circ$  of latitudinal width where precipitating electrons increase and then decrease in average energy with latitude. The spectrum of precipitating electrons in inverted V events indicate that plasma-sheet type electrons have been accelerated by a few kV.

34. Lysak, R. L., and Hudson, M. K. (1979) Coherent anomalous resistivity in the region of electrostatic shocks, Geophys. Res. Letters 6(No. 8):661-663.

Since there are parallel electric fields associated with shocks, especially in regions of upward current, the region of the shock would seem to be a good candidate to the source of inverted V events. Unfortunately, the latitudinal scale of the two features do not match. Since the shocks on 6 September 1976 are embedded in a broad inverted V event extending from 0255 to 0258 UT (Mizera et al<sup>27</sup>), there may be some relationship between the two. Since the particle data indicates parallel electric fields throughout the region of the inverted V, the shocks may be only a local grouping of latitudinally broad sets of V- or S-shaped equipotentials. If all of the equipotentials between 69° and 71° that are related to parallel electric fields were V-shaped, then the large-scale electric field observed at S3-3 altitude would be systematically larger than at S3-2 altitude after scaling for the divergence of the field lines. Since the electric fields are approximately equal despite the small-scale discrepancies, some of the parallel electric fields in the region of the inverted V should be due to S-shaped potentials.

The regions of strong perpendicular electric fields or shocks are of the same small, latitudinal scale as discrete arcs, and it is tempting to say that shocks with parallel electric fields produce discrete arcs. Burke et al<sup>20</sup> shows that discrete arcs are located in regions of enhanced upward current with latitudinal widths of 0.1° to 0.5° within the region 1 current sheet in the evening sector. If, then, shocks produce discrete arcs, there should be a relationship between shocks and field-aligned currents. Comparing regions of shocks observed by the S3-3 satellite with S3-3 magnetometer data, we do not find any relationship. This may be due to two factors: First, since some shocks do not have a field-aligned electric field region pointed upward, there may not be any relationship between these shocks and field-aligned currents. Second, a latitudinal scale of 0.5° is the limit of the resolution of the S3-3 magnetometer and many regions of enhanced upward current may go unnoticed. Comparing regions of shocks observed by the S3-3 satellite with S3-2 magnetometer data, we again do not find any relationship. This is due in part to the difference in local time between the two satellite paths and our inability to map currents from high to low altitudes with an accuracy of better than 0.5°. Hardy et al<sup>29</sup> compared electric field data with magnetometer data from S3-2 for 6 September 1976 and found a large field-aligned current with a latitudinal extent of ~2 km near the shock shown in Figure 4. Magnetometer data for this current sheet is not shown in Figure 3 because its scale is so small that it would look like a smudge on the page. There are no similar small-scale, large-magnitude current sheets in any other S3-2 magnetometer data near S3-3 shocks.

If electrostatic shock regions do not significantly affect the large scale, field-aligned currents, are those currents uniform from 8000 km to the auroral electrojet? The data tends to indicate that often the currents do not vary with height, as shown by the comparisons of 3 September 1976, 6 September 1976 (except near

the shock), and 20 September 1977, but sometimes they do. The possibility exists that the observed variations are really temporal instead of spatial because the observations are not exactly simultaneous. While temporal variations can never be ruled out as long as the observations are not exactly simultaneous and coplanar, we believe that temporal variations are not the only effect found because all three cases shown (15 October 1976, 19 September 1976, and 12 September 1976) have more field-aligned current flowing at high altitudes than at low altitudes. Temporal variations should yield some cases where more current was observed at low altitudes than at high altitudes; however, the statistics are not conclusive with only three examples. More importantly, the ground-based magnetometer data have been checked for signs of temporal variations. On 12 September 1976, the passes presented here occurred during a quiet period between two small, isolated substorms. On 19 September 1976, the observations were made during a phase of a substorm when the electrojet was changing slowly. On 15 October 1976, the electrojet was disturbed and the observations presented in Figure 6 may indeed be dominated by temporal variations. The possibility also exists that the difference in the observations are caused by a magnetic local time dependence of the field-aligned currents. For example, Iijima and Potemra<sup>30</sup> showed that the average current density at 1700 MLT is  $\sim 1.3$  times that at 1800 MLT. If we apply a magnetic local time correction factor of  $\sim 1.3$  to the data on 12 September 1976 (Figure 11), we find that there is an even larger discrepancy between the S3-3 and S3-2 observations. In the case of 15 October 1976, the magnetic local time factor is insufficient to account for all discrepancies, and in the case of 19 September 1976, there is no significant difference in the magnetic local time. That leaves, in at least two of the cases, the problem of determining where the excess current observed at high altitudes went to. To answer this question, we have done a detailed analysis of the currents observed on 19 September 1976. This day was chosen because of the closeness in local time and in universal time of the passage of the two satellites, and the lack of large changes in the auroral electrojet as determined by the Greenland magnetometer chain.

The analysis of 19 September 1976 is shown in Figure 11 as a wiring diagram. The total sheet current observed by each satellite in each region is shown as an element of the circuit, assuming that the field-aligned current consists of semi-infinite sheets. Region 2 has been divided into two regions: One from  $71^\circ$  to  $68^\circ$  where both satellites observed a field-aligned current, and the other from  $68^\circ$  to  $65^\circ$  where only S3-3 observed a significant field-aligned current. The result of this wiring diagram analysis is the fact that a considerable amount of current must have been flowing across field lines between 300 km and 3000 km altitude.

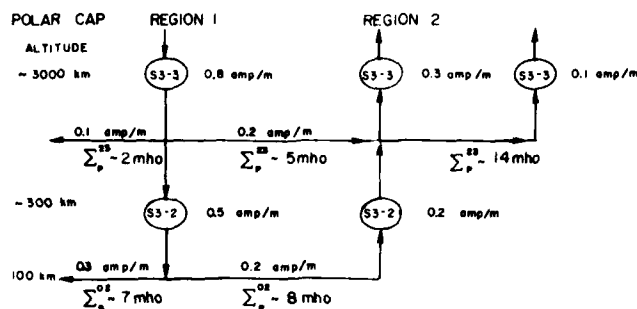


Figure 11. A Schematic Diagram of the Currents Observed by S3-3 and S3-2 on 19 September 1976. The horizontal components of the currents are determined from current conservation. The Pedersen conductivities are estimated from the horizontal currents and the observed electric fields

The magnitude of the Pedersen Currents in Figure 11 are obtained from the difference between the high- and low-altitude field-aligned currents and ignoring any east-west currents. The height integrated conductivities are calculated by dividing the horizontal currents by the average electric-field strength. The uncertainty of the horizontal currents is 25%. The uncertainty of the height integrated conductivity between the electrojet and S3-2 ( $\Sigma^{02}$ ) and between S3-2 and S3-3 ( $\Sigma^{23}$ ) is 50% in region 1 and 100% in region 2 and at the polar cap. Since the classical Pedersen conductivity between 300 km and ~500 km is small and above ~500 km the classical Pedersen conductivity is zero, the height integrated conductivities between the two satellites are larger than expected by orders of magnitude.

In the case of 6 September, which has been studied in detail by Mizera et al.<sup>27</sup> on S3-3, we can argue that the similarity of the electrostatic shocks implies that large wave fluctuations such as those detected on S3-3 were present throughout the altitude range from 1000 to 8000 km. This in turn implies that a region of strong wave turbulence must often exist in the auroral zone ionosphere, the order of an Earth radius in altitude extent. Turbulent electrostatic waves are known to strongly scatter plasma constituents and cause anomalous diffusion in laboratory plasmas. Bohm diffusion is an example of such a process, and Drummond and Rosenbluth<sup>35</sup> suggested ion cyclotron waves as the source for this phenomenon. In collision-dominated media, diffusion and conductivity are both determined by the rate at which particles collide. In the collisionless media, wave-particle interactions may take the place of collisions in determining these macroscopic transport

35. Drummond, W. E., and Rosenbluth, M. N. (1962) Anomalous diffusion arising from micro-instabilities in a plasma, *Phys. Fluids* 5:1507.

coefficients. Since ion cyclotron waves are a common feature of the topside ionosphere (Kintner et al<sup>36,37</sup>; Mizera et al<sup>27</sup>) and since such waves have been related to cross-field diffusion in the laboratory, it is tempting to hypothesize that anomalous perpendicular resistivity exists in the Earth's magnetosphere.

A calculation of anomalous perpendicular resistivity is beyond the scope of this report. We can, however, make some estimates of the required "effective" collision frequency,  $\nu'$ , necessary to support the observed differences in field-aligned current. To make any progress at all, we assume that  $\nu$  is proportional to the local ion cyclotron frequency, that is,  $\nu' = r\Omega$  with  $r$  a constant. The circuit diagram in Figure 11 shows that the height-integrated conductivity,  $\Sigma$ , in the E region ionosphere and in the high-altitude ionosphere are comparable. We can express the Pedersen conductivity as

$$\sigma_p = \frac{ne^2\nu}{m_i\Omega^2}, \quad (4)$$

where  $n$  is the electron density,  $e$  the electron charge,  $\nu$  the collision frequency (either collisional or effective),  $m_i$  the ion mass, and  $\Omega$  the ion gyro frequency. Integrating over the two altitude ranges, setting the height-integrated conductivities equal, and assuming  $\nu' = R\Omega$  yields

$$\int_{\text{E-region}} \frac{ne^2\nu}{m_i\Omega^2} dz = \int_{\text{topside}} \frac{ne^2}{m_i\Omega} dz. \quad (5)$$

To evaluate  $R$  we further assume that the electron density and magnetic field strength are proportional in the topside ionosphere. Then the  $z$  dependence cancels and the integral is equal to the length of the unstable topside region,  $L$ , times the value of  $ne/B$  at the base of the region:

$$R = \frac{\Sigma_p B}{ne L}. \quad (6)$$

36. Kintner, P.M., Kelley, M.C., and Mozer, F.S. (1978) Electrostatic hydrogen cyclotron waves near one earth radius in the polar magnetosphere, Geophys. Res. Letters 5:139.
37. Kintner, P.M., Kelley, M.C., Sharp, R.D., Ghielmetti, A.G., Temerin, M., Cattell, C.A., Mizera, P., and Fennell, J. (1979) Simultaneous observations of energetic (keV) upstreaming ions and EHC waves, J. Geophys. Res. 84:720.

For  $\Sigma_p = 5 \text{ mho}$ ,  $n \sim 10^4 \text{ cm}^{-3}$ ,  $L = 1 R_e$ , and  $B = 0.4 \times 10^{-4} \text{ T}$ , we have  $R \sim 0.02$ . If we included a realistic height-dependence of  $B/n$ , then  $R \sim 0.1$ . Thus an effective collision frequency on the order of a few percent of the ion cyclotron frequency would explain the present observation. This seems to be a reasonable requirement for the wave-particle interaction, even though we do not understand the details of the mechanism.

Gary<sup>38</sup> has made a detailed study of various wave-particle interactions and their affect on "anomalous" transport coefficients. For the current-driven ion-cyclotron instability, he found that the condition for anomalous perpendicular conductivity is:

$$\Omega/\sigma_p = 4\sqrt{2} \pi^{3/2} (4/5)^4 (m_e/m_i)^{1/2} \frac{(T_e/T_i)^{1/2}}{(1 + (T_i/T_e))} (\Omega/\omega)^2, \quad (7)$$

where  $4 \leq T_e/T_i \leq 10$ , and  $\omega$  is the ion plasma frequency. Defining an effective collision frequency using Eq. (4), we obtain

$$\nu' = \frac{(5/4)^4}{\sqrt{2\pi}} (m_i/m_e)^{1/2} \frac{1 + T_i/T_e}{(T_e/T_i)^{1/2}} \Omega. \quad (8)$$

This represents an effective collision frequency that is considerably greater than the ion cyclotron frequency and is more than adequate to explain the present observation. In order to have a net current, there must be a net momentum across the field lines. This is possible if the wave vectors in the instability region are anisotropic, or if there is momentum transfer between particle species by way of the wave field.

Another possibility is that current is diverted across magnetic field lines by time-varying electric fields. This could occur by having the plasma convect from the night sector toward the day sector through a region of increasing meridional electric field. In the rest frame of the plasma, this would appear as a time-varying field. The current is given by

$$\underline{J} = -\epsilon \frac{d}{dt} \underline{E}$$

where  $\epsilon$  is the low-frequency dielectric permittivity. We can estimate the magnitude of this current as follows:

38. Gary, S. P. (1980) Wave particle transport from electrostatic instabilities, Phys. Fluids 23(No. 6):1193-1204.



Let  $\tau$  be the characteristic time scale for the electric field change. Then,  $J = (\epsilon/\tau)E$  and we have an effective conductivity of  $(\epsilon/\tau)$ . The effective height-integrated conductivity is then  $\Sigma' = \epsilon L/\tau$ , where  $L$  is the altitude range between S3-2 and S3-3. The dielectric constant is  $(c/V_A)^2 \epsilon_0$ , where  $V_A$  is the Alfvén speed and  $\epsilon_0$  is the permittivity of a vacuum. An upper limit for  $\epsilon$  is  $10^5 \epsilon_0$  which corresponds to an Alfvén speed of 1000 km/sec. If the electric field change also takes place over a distance of the order of  $L$  and a mean  $\underline{E} \times \underline{B}$  drift of 2000 m/sec, then  $\Sigma'$  is  $2 \times 10^{-3}$  mho. This is much too small and any other reasonable selection of parameters would also yield values of  $\Sigma$  which are much too small.

Another possibility is that current diverted across magnetic field lines by time-varying electric fields in the reference frame of the current particles as they travel up or down the field lines. The varying electric field in this case would be the strong dc electric field associated with a shock region. This mechanism could redistribute currents by the latitudinal width of the shock ( $\leq 1^\circ$ ), but the net field-aligned current flowing into or out of the ionosphere would be unchanged.

A third alternative is that current is diverted across field lines by  $\nabla E \times B$  forces. In the geometry of the shocks, the largest gradient is in the north-south direction since shocks, like auroral arcs, are extensive in the east-west direction. Thus the  $\nabla E \times B$  current flows in the east-west direction with a magnitude given by

$$j_{EW} \approx 2 ne \frac{E}{B} \frac{r_L}{r_E} \approx 8/3 \times 10^{-7} \left( \frac{r_L}{r_E} \right) \text{ A/m}^2,$$

where  $r_L$  is the ion gyroradius and  $r_E$  is the electric-field scale length. A typical value for  $r_L/r_E$  for S3-3 is 0.03, so  $j_{EW} \approx 8 \times 10^{-9} \text{ A/m}^2$ . This is much smaller than the field-aligned current. Also, there should be two  $\nabla E \times B$  currents, one on each side of the large electric field, of approximate equal magnitude and of opposite direction. Thus it is not possible to divert a net current into this current system.

We conclude that anomalous perpendicular conductivity is the most likely explanation for two of the three cases where the large scale, field-aligned current systems appear to be different at the two satellite altitudes. Of course, other effects including temporal variations cannot be ruled out. If there is an anomalous perpendicular conductivity, the details of the wave-particle collision process is beyond the scope of this report, but it must include momentum transfer.

## 5. CONCLUSIONS

We have presented electric and magnetic-field data from the S3-2 and S3-3 satellites when they were nearly simultaneously on approximately the same field lines in the auroral zone at two widely different altitudes. We have found that most of the latitudinally narrow regions of strong  $E_1$  observed by S3-3 are indeed confined to high altitudes ( $h \geq 1500$  km), as was previously suggested by an altitude variation of shock occurrences as seen by S3-3 and suggested by ion and electron particle distribution functions. There are some clues in the data to reason for the termination of the shocks, but we cannot conclusively state the cause. While electrostatic shock may be due to current-driven instability, the majority of field-aligned current is carried outside the region of the shocks. We found several cases where the field-aligned currents were different at different altitudes. Although we cannot completely rule out other effects such as temporal and local time variations, we argue that there are altitude variations of the field-aligned current. If there are, an anomalous Pederson conductivity seems to be the best candidate for finding the cause of the altitude variation of the field-aligned current.

## References

1. Horwitz, J. L., Doupnik, J. R., Banks, D. M., Kamide, Y., and Akasofu, S. -I. (1978) The latitudinal distribution of auroral zone electric fields and ground magnetic perturbations and their response to variations in the interplanetary magnetic field, J. Geophys. Res. 83:80.
2. Evans, J. V., Holt, J. M., and Ward, R. H. (1979) Millstone Hill incoherent scatter observations of auroral convection over  $60^\circ \leq T \leq 75^\circ$ , 1., Observing and data reduction procedures, J. Geophys. Res. 84:7059.
3. Haerendel, G., Rieger, E., Valenzuela, A., and Wescott, H. (1976) First observation of electrostatic acceleration of barium ions into the magnetosphere, in European Programmes on Sounding-Rocket and Balloon Research in the Auroral Zone, ESA-SP115, European Space Agency, Neuilly, France, August.
4. Westcott, E. M., Stenbaek-Nielsen, H. C., Hallinan, T. J., Davis, T. N., and Peek, H. M. (1976) The skylab barium plasma injection experiments, 2. Evidence for a double layer 81(No. 25):4495-4502.
5. Westcott, E. M., Stenbaek-Nielsen, H. C., Davis, T. N., Jeffries, R. A., and Roach, W. H. (1978) The Tordo 1 polar cusp barium plasma injection experiment, J. Geophys. Res. 83(A4):1565-1575.
6. Mizera, P. F., and Fennell, J. F. (1977) Signatures of electric fields from high and low altitude particle distributions, Geophys. Res. Letters 4(No. 8):311-314.
7. Croley, D. R., Mizera, P. F., and Fennell, J. F. (1978) Signature of a parallel electric field in ion and electron distributions in velocity space, J. Geophys. Res. 83(A6):2701-2705.
8. Shelley, E. G., Sharp, R. D., and Johnson, R. G. (1976) Satellite observations of an ionospheric acceleration mechanism, Geophys. Res. Letters 3(No. 11):654-656.
9. Sharp, R. D., Johnson, R. G., and Shelley, E. G. (1977) Observation of an ionospheric acceleration mechanism producing energetic (keV) ions primarily normal to the geomagnetic field direction, J. Geophys. Res. 82(No. 22):3324-3328.

## References

10. Ghielmetti, A.C., Johnson, R.G., Sharp, R.D., and Shelley, E.G. (1978) The latitudinal, diurnal and altitudinal distribution of upflowing energetic ions of ionospheric origin, Geophys. Res. Letters 5(No. 1):58-62.
11. Sharp, R.D., Johnson, R.G., and Shelley, E.C. (1979) Energetic particle measurements from within ionospheric structures responsible for auroral acceleration processes, J. Geophys. Res. 84(A2):480-488.
12. Mozer, F.S., Cattell, C.A., Hudson, M.K., Dysak, R.I., Tenerin, M., and Torbert, R.B. (1980) Satellite measurements and theories of low altitude auroral particle acceleration, Space Sci. Rev., in press.
13. Gorney, D.J., Clarke, A., Croley, D., Fennell, J., Luhmann, J., and Mizera, P. (1980) The distribution of ion beams and conics below 8000 km, submitted to J. Geophys. Res.
14. Mozer, F.S., Carlson, C.W., Hudson, M.K., Torbert, R.B., Parady, B., Yetteau, J., and Kelley, M.C. (1977) Observations of paired electrostatic shocks in the polar magnetospheres, Phys. Rev. Letters 38:292-294.
15. Swift, D.W. (1975) On the formation of auroral arcs and acceleration of auroral electrons, J. Geophys. Res. 80(No. 16):2096-2108.
16. Swift, D.W. (1976) The equipotential model for auroral arcs, 2. Numerical solutions, J. Geophys. Res. 81(No. 22):3935-3943.
17. Mozer, F.S., and Torbert, R.B. (1980) An average parallel electric field deduced from the latitude and altitude variations of the perpendicular electric field below 8000 kilometers, Geophys. Res. Letters 7:219-221.
18. Gonzales, C.A., Kelley, M.C., Carpenter, D.I., Miller, T.R., and Ward, R.H., (1980) Simultaneous measurements of ionospheric and magnetospheric electric fields in the outer plasmasphere, Geophys. Res. Letters 7(No. 7):517-520.
19. Kan, J.R., and Lee, I.C. (1980) Double layer criterion on the altitude of the auroral acceleration region, Geophys. Res. Letters 7(No. 6):429-432.
20. Burke, W.J., Hardy, D.A., Rich, F.J., Kelley, M.C., Smiddy, M., Shuman, B., Sagalyn, R.C., Vancour, R.P., Wildman, P.J.L., and Lai, S.T. (1980) Electrodynamical structure of the late evening sector of the auroral zone, J. Geophys. Res. 85(A3):1179-1193.
21. Mozer, F.S., Cattell, C.A., Tenerin, M., Torbert, R.B., Vonglinski, S., Woldorf, M., and Wygant, J. (1979) The dc and ac electric field, plasma density, plasma temperature and field aligned current experiments on the S3-3 satellite, J. Geophys. Res. 84(A10):5875-5884.
22. Mozer, F.S. (1970) Electric field mapping in the ionosphere at the equatorial plane, Planet. Space Sci. 18:259-263.
23. Smiddy, M., Burke, W.J., Kelley, M.C., Saflekos, N.A., Gussenhovorn, M.S., Hardy, D.A., and Rich, F.J. (1980) Effects of high latitude conductivity on observed convection electric fields and Birkland Currents, J. Geophys. Res. 85(A12):6811-6818.
24. Torbert, R.B., and Mozer F.W. (1978) Electrostatic shocks as the source of discrete auroral arcs, Geophys. Res. Letters 5(No. 2):135-138.
25. Mozer, F.W. (1980) ISEE-1 observations of electrostatic shocks on auroral zone field lines between 2.5 and 7 Earth Radii, submitted to Geophys. Res. Letters.

## References

26. Hudson, M.K., and Mozer, F.W. (1978) Electrostatic shocks, double layers, and anomalous resistivity in the magnetosphere, Geophys. Res. Letters 5:131.
27. Mizera, P.F., Fennell, J.F., Croley, D.R., Jr., Vampola, A.L., Mozer, F.S., Torbert, R.B., Tenerin, M., Lysak, R., Hudson, M., Cattell, C.A., Johnson, R.J., Sharp, R.D., Ghielmetti, A., and Kintner, P.M. (1980) The aurora inferred from S3-3 particles and fields, submitted to J. Geophys. Res.
28. Smiddy, M., Kelley, M.C., Burke, W., Rich, F., Sagalyn, R., Shuman, B., Mays, R., and Lai, S. (1977) Intense pole-ward directed electric fields near the ionospheric projection of the plasmopause, Geophys. Res. Letters 4:543.
29. Hardy, D.A., Burke, W.J., Rich, F., and Kelley, M.C. (1980) Intense Birkeland Current structures observed in the vicinity of latitudinally narrow dc electric field variations, to be submitted to J. Geophys. Res.
30. Iijime, T., and Potemra, T.A. (1976) The amplitude distribution of field-aligned currents at northern high latitudes observed by TRIAD, J. Geophys. Res. 81(No. 13):2165-2174.
31. Harel, M., Wolf, R.A., Reiff, P.H., Spiro, R.W., Burke, W.J., Rich, R.J., and Smiddy, M. (1980) Quantitative simulation of a magnetospheric substorm, 1. Model logic and overview, submitted to J. Geophys. Res.
32. Harel, M., Wolf, R.A., Spiro, R.W., Reiff, P.H., Chen, C.K., Burke, W.J., Rich, F.J., and Smiddy, M. (1980) Quantitative simulation of a magnetospheric substorm, 2. Comparison with observations, submitted to J. Geophys. Res.
33. Cattell, C., Lysak, R., Torbert, R.B., and Mozer, F.S. (1979) Observations of differences between regions of current flowing into and out of the ionosphere, Geophys. Res. Letters 6(No. 7):621-624.
34. Lysak, R.L., and Hudson, M.K. (1979) Coherent anomalous resistivity in the region of electrostatic shocks, Geophys. Res. Letters 6(No. 8):661-663.
35. Drummond, W.E., and Rosenbluth, M.N. (1962) Anomalous diffusion arising from micro-instabilities in a plasma, Phys. Fluids 5:1507.
36. Kintner, P.M., Kelley, M.C., and Mozer, F.S. (1978) Electrostatic hydrogen cyclotron waves near one earth radius in the polar magnetosphere, Geophys. Res. Letters 5:139.
37. Kintner, P.M., Kelley, M.C., Sharp, R.D., Ghielmetti, A.G., Tenerin, M., Cattell, C.A., Mizera, P., and Fennell, J. (1979) Simultaneous observations of energetic (keV) upstreaming ions and EHC waves, J. Geophys. Res. 84:720.
38. Gary, S.P. (1980) Wave particle transport from electrostatic instabilities, Phys. Fluids 23(No. 6):1193-1204.

